AMERICAN SOCIETY FOR MICROBIOLOGY | Applied and Environmental Microbiology®

EVOLUTIONARY AND GENOMIC MICROBIOLOGY

Enterococcus faecalis OG1RF Evolution at Low pH Selects Fusidate-Sensitive Mutants in Elongation Factor G and at High pH Selects Defects in Phosphate Transport

Bailey A. Fitzgerald,[a] Ayman Wadud,[a] Zachary Slimak,[a] Joan L. Slonczewski[a]

[a]Department of Biology, Kenyon College, Gambier, Ohio, USA

Bailey A. Fitzgerald and Ayman Wadud contributed equally to this study and are co-first authors. The author order was determined by consensus of all authors.

ABSTRACT *Enterococcus* bacteria inhabit human and soil environments that show a wide range of pH values. Strains include commensals as well as antibiotic-resistant pathogens. We investigated the adaptation to pH stress in *E. faecalis* OG1RF by conducting experimental evolution under acidic (pH 4.8), neutral pH (pH 7.0), and basic (pH 9.0) conditions. A serial planktonic culture was performed for 500 generations and in a high-pH biofilm culture for 4 serial bead transfers. Nearly all of the mutations led to nonsynonomous codons, indicating adaptive selection. All of the acid-adapted clones from the planktonic culture showed a mutation in *fusA* (encoding elongation factor G). The acid-adapted *fusA* mutants had a trade-off of decreased resistance to fusidic acid (fusidate). All of the base-adapted clones from the planktonic cultures as well as some from the biofilm-adapted cultures showed mutations that affected the Pst phosphate ABC transporter (*pstA*, *pstB*, *pstB2*, *pstC*) and *pyrR* (pyrimidine biosynthesis regulator/uracil phosphoribosyltransferase). The biofilm cultures produced small-size colonies on brain heart infusion agar. These variants each contained a single mutation in *pstB2*, *pstC*, or *pyrR*. The *pst* and *pyrR* mutants outgrew the ancestral strain at pH 9.2, with a trade-off of lower growth at pH 4.8. Additional genes that had a mutation in multiple clones that evolved at high pH (but not at low pH) include *opp1BCDF* (oligopeptide ABC transporter), *ccpA* (catabolite control protein A), and *ftsZ* (septation protein). Overall, the experimental evolution of *E. faecalis* showed a strong pH dependence, favoring the fusidate-sensitive elongation factor G modification at low pH and the loss of phosphate transport genes at high pH.

IMPORTANCE *E. faecalis* bacteria are found in dental biofilms, where they experience low pH as a result of fermentative metabolism. Thus, the effect of pH on antibiotic resistance has clinical importance. The loss of fusidate resistance is notable for OG1RF strains in which fusidate resistance is assumed to be a stable genetic marker. In endodontal infections, enterococci can resist calcium hydroxide therapy that generates extremely high pH values. In other environments, such as the soil and plant rhizosphere, enterococci experience acidification that is associated with climate change. Thus, the pH modulation of natural selection in enterococci is important for human health as well as for understanding soil environments.

KEYWORDS *Enterococcus*, acid stress, antibiotic resistance, base stress, evolution, fusidic acid, pH stress, phosphate transport, stress response

Enterococcus faecalis are Gram-positive fermenter bacteria that are found in a wide range of habitats, including dental biofilms and the gastrointestinal tract of humans (1–4) as well as soil and plants (5). Pathogenic strains cause a variety of infections throughout the body, which are of special concern in hospitals due to the acquired vancomycin resistance in certain strains and an intrinsic antibiotic resistance

Editor Christopher A. Elkins, Centers for Disease Control and Prevention

Address correspondence to Joan L. Slonczewski, slonczewski@kenyon.edu.

The authors declare no conflict of interest.

Received 21 March 2023
Accepted 15 May 2023

to numerous other antibiotics (6). *Enterococcus* species are known for their abilities to tolerate a wide range of conditions such as salinity, temperature, and pH (6–9). Survival at low pH is important for enteric infections, and survival at high pH is relevant to dental biofilms that are treated with calcium hydroxide pastes (10, 11). Multidrug-resistant enterococci are isolated from environmental sources, such as soil (12) and the digestive microbiomes of farm animals, insects, and nematodes (13). At the same time, environmental enterococci with wide-ranging stress resistance offer potential benefits, such as tolerance of toxic metals (14) and probiotics (15).

Surprisingly, little is known about the genetics of enterococcal adaptation to acids or bases. In *E. faecium*, acid shock leads to metabolomic changes, such as the elevated production of dipeptides (16). Acid stress in *Enterococcus* has been studied as a part of general stress responses (17–19). At high pH values, such as in the presence of the dental application of calcium hydroxide, *Enterococcus* survival requires the maintenance of the proton motive force (20). The cellular effects of high pH include changes in morphology (21), metabolism, and protein synthesis (22, 23).

In Gram-negative bacteria, acid adaptation is associated with fitness tradeoffs, such as the loss of antibiotic resistance. *Escherichia coli* K-12 experimental evolution at a low pH (24, 25) or in the presence of benzoic acid (26, 27) leads to the loss of genes encoding multidrug transporters that are powered by the proton-motive force. Therefore, it was of interest to explore the pH stress adaptation and fitness tradeoffs in a Gram-positive model organism.

We investigated the genetics of pH stress in the model organism *Enterococcus faecalis* OG1RF (2) by means of the experimental evolution of planktonic and biofilm cultures. For comparison, in *E. coli*, experimental evolution in an acid or base yields mutations in several stress response genes, such as amino-acid decarboxylases (24, 25, 28) and acid-resistance regulators (29). In *E. faecalis,* pH stress is crucial for biofilm formation and endodontic infections (20, 30). Experimental evolution by serial bead transfer is a method used to investigate stress effects in biofilms. Bead-transfer experiments yield informative genetic variants in other environmental bacteria, such as *Pseudomonas* and *Burkholderia* species (31, 32). In *Enterococcus* species, experimental evolution has been applied to studies of virulence and antimicrobial susceptibility (33, 34) but not to more fundamental stress factors, such as pH.

We found that experimental evolution yields pH-adaptative mutations in several genes, notably the encoding elongation factor G (*fusA*) at low pH andthe phosphate ABC transporter (*pstABC*) at high pH. Mutations in *fusA* may confer resistance to fusidic acid (35, 36), but the OG1RF background strain is assumed to have a stable fusidate-resistance phenotype that is used for genetic selection. Thus, it is notable that in our experiments, just a few hundred generations led to strains that lost fusidate resistance. The *pts* loci are associated with virulence (37, 38). In our biofilm-evolved strains, base-selected mutations in *pstABC* and in *pyrR* (pyrimidine biosynthesis regulator) led to small-colony growth, a phenotype class that is associated with virulence in clinical strains (39, 40).

RESULTS

Experimental evolution of acid-adapted and base-adapted mutants. The experimental evolution of *E. faecalis* OG1RF was conducted via microplate serial dilutions at 1:250, as described under Materials and Methods. Eight evolving populations were maintained in brain heart infusion (BHI) that was buffered at three individual pH values: pH 4.8, pH 7.0, and pH 9.0. After 500 generations, one isolate from each population was resequenced for comparison with the OG1RF reference (2), using the *breseq* resequencing pipeline (41, 42).

The resequenced clones had a range of one to five mutations per clone. The mutations predicted were nearly all point mutations or small deletions (Fig. 1). Only one deletion encompassed more than one gene (genes encoding catechol 2,3 dioxygenase and a multidrug ABC transporter in clone C06). Overall, the ratio of nonsynonymous to synonymous codon changes was extremely high, with only 1 silent mutation out of 48. The

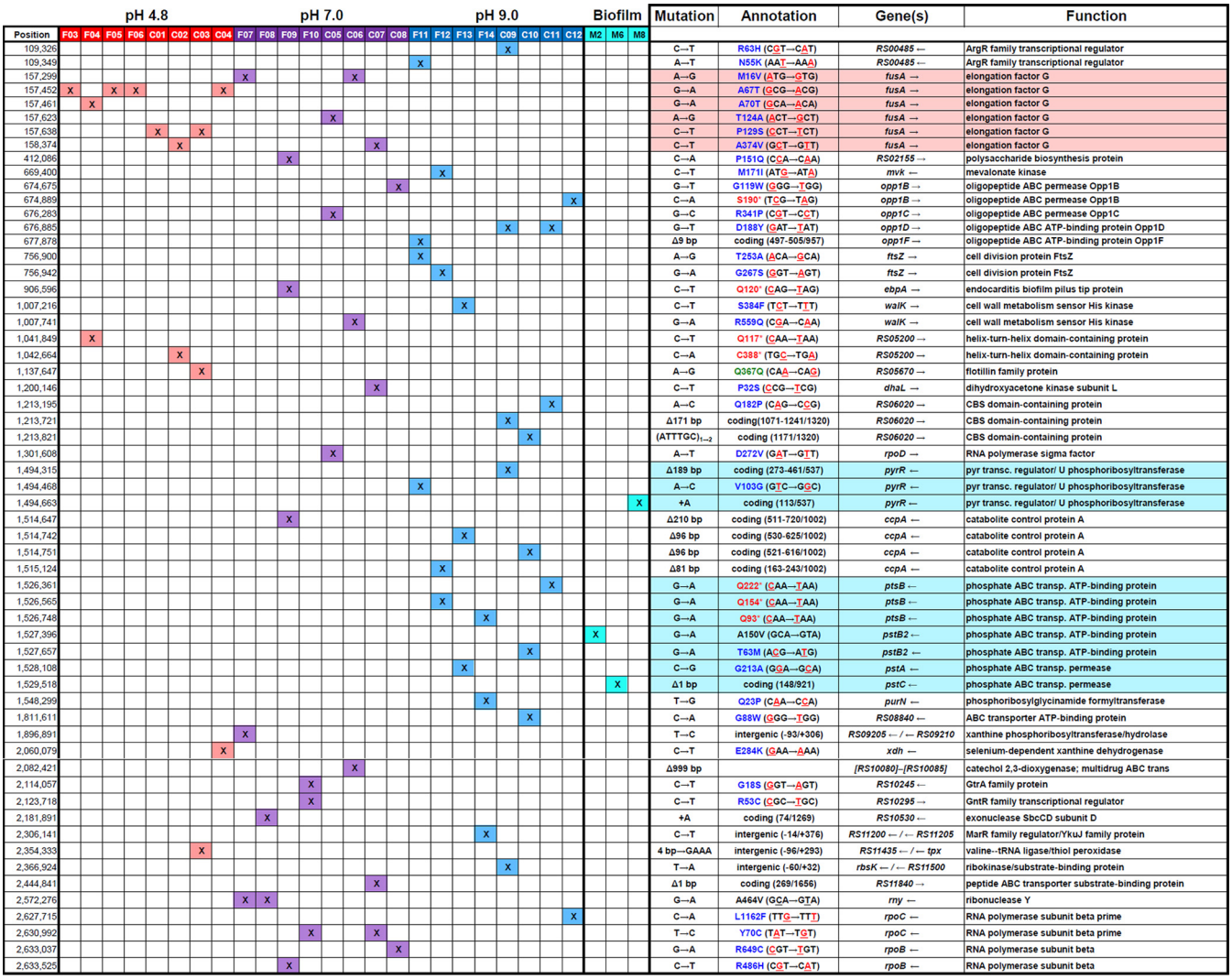

Position	F03	F04	F05	F06	C01	C02	C03	C04	F07	F08	F09	F10	C05	C06	C07	C08	F11	F12	F13	F14	C09	C10	C11	C12	M2	M6	M8	Mutation	Annotation	Gene(s)	Function
109,326																					X							C⟶T	R63H (CGT⟶CAT)	*RS00485* ←	ArgR family transcriptional regulator
109,349																	X											A⟶T	N55K (AAT⟶AAA)	*RS00485* ←	ArgR family transcriptional regulator
157,299									X				X															A⟶G	M16V (ATG⟶GTG)	*fusA* →	elongation factor G
157,452	X		X	X				X																				G⟶A	A67T (GCG⟶ACG)	*fusA* →	elongation factor G
157,461		X																										G⟶A	A70T (GCA⟶ACA)	*fusA* →	elongation factor G
157,623													X															A⟶G	T124A (ACT⟶GCT)	*fusA* →	elongation factor G
157,638					X		X																					C⟶T	P129S (CCT⟶TCT)	*fusA* →	elongation factor G
158,374						X									X													C⟶T	A374V (GCT⟶GTT)	*fusA* →	elongation factor G
412,086											X																	C⟶A	P151Q (CCA⟶CAA)	*RS02155* →	polysaccharide biosynthesis protein
669,400																		X										C⟶T	M171I (ATG⟶ATA)	*mvk* ←	mevalonate kinase
674,675																X												G⟶T	G119W (GGG⟶TGG)	*opp1B* →	oligopeptide ABC permease Opp1B
674,889																								X				C⟶A	S190* (TCG⟶TAG)	*opp1B* →	oligopeptide ABC permease Opp1B
676,283													X															G⟶C	R341P (CGT⟶CCT)	*opp1C* →	oligopeptide ABC permease Opp1C
676,885																					X		X					G⟶T	D188Y (GAT⟶TAT)	*opp1D* →	oligopeptide ABC ATP-binding protein Opp1D
677,878																	X											Δ9 bp	coding (497-505/957)	*opp1F* →	oligopeptide ABC ATP-binding protein Opp1F
756,900																	X											A⟶G	T253A (ACA⟶GCA)	*ftsZ* →	cell division protein FtsZ
756,942																		X										G⟶A	G267S (GGT⟶AGT)	*ftsZ* →	cell division protein FtsZ
906,596											X																	C⟶T	Q120* (CAG⟶TAG)	*ebpA* →	endocarditis biofilm pilus tip protein
1,007,216																			X									C⟶T	S384F (TCT⟶TTT)	*walK* →	cell wall metabolism sensor His kinase
1,007,741													X															G⟶A	R559Q (CGA⟶CAA)	*walK* →	cell wall metabolism sensor His kinase
1,041,849		X																										C⟶T	Q117* (CAA⟶TAA)	*RS05200* →	helix-turn-helix domain-containing protein
1,042,664						X																						C⟶A	C388* (TGC⟶TGA)	*RS05200* →	helix-turn-helix domain-containing protein
1,137,647							X																					A⟶G	Q367Q (CAA⟶CAG)	*RS05670* →	flotillin family protein
1,200,146															X													C⟶T	P32S (CCG⟶TCG)	*dhaL* →	dihydroxyacetone kinase subunit L
1,213,195																								X				A⟶C	Q182P (CAG⟶CCG)	*RS06020* →	CBS domain-containing protein
1,213,721																					X							Δ171 bp	coding(1071-1241/1320)	*RS06020* →	CBS domain-containing protein
1,213,821																						X						(ATTTGC)$_{1\rightarrow2}$	coding (1171/1320)	*RS06020* →	CBS domain-containing protein
1,301,608													X															A⟶T	D272V (GAT⟶GTT)	*rpoD* →	RNA polymerase sigma factor
1,494,315																					X							Δ189 bp	coding (273-461/537)	*pyrR* ←	pyr transc. regulator/ U phosphoribosyltransferase
1,494,468																	X											A⟶C	V103G (GTC⟶GGC)	*pyrR* ←	pyr transc. regulator/ U phosphoribosyltransferase
1,494,663																											X	+A	coding (113/537)	*pyrR* ←	pyr transc. regulator/ U phosphoribosyltransferase
1,514,647											X																	Δ210 bp	coding (511-720/1002)	*ccpA* ←	catabolite control protein A
1,514,742																			X									Δ96 bp	coding (530-625/1002)	*ccpA* ←	catabolite control protein A
1,514,751																						X						Δ96 bp	coding (521-616/1002)	*ccpA* ←	catabolite control protein A
1,515,124																		X										Δ81 bp	coding (163-243/1002)	*ccpA* ←	catabolite control protein A
1,526,361																								X				G⟶A	Q222* (CAA⟶TAA)	*ptsB* ←	phosphate ABC transp. ATP-binding protein
1,526,565																		X										G⟶A	Q154* (CAA⟶TAA)	*ptsB* ←	phosphate ABC transp. ATP-binding protein
1,526,748																				X								G⟶A	Q93* (CAA⟶TAA)	*ptsB* ←	phosphate ABC transp. ATP-binding protein
1,527,396																									X			G⟶A	A150V (GCA⟶GTA)	*pstB2* ←	phosphate ABC transp. ATP-binding protein
1,527,657																						X						G⟶A	T63M (ACG⟶ATG)	*pstB2* ←	phosphate ABC transp. ATP-binding protein
1,528,108																			X									C⟶G	G213A (GGA⟶GCA)	*pstA* ←	phosphate ABC transp. permease
1,529,518																										X		Δ1 bp	coding (148/921)	*pstC* ←	phosphate ABC transp. permease
1,548,299																				X								T⟶G	Q23P (CAA⟶CCA)	*purN* ←	phosphoribosylglycinamide formyltransferase
1,811,611																						X						C⟶A	G88W (GGG⟶TGG)	*RS08840* ←	ABC transporter ATP-binding protein
1,896,891									X																			T⟶C	intergenic (-93/+306)	*RS09205* ← / ← *RS09210*	xanthine phosphoribosyltransferase/hydrolase
2,060,079								X																				C⟶T	E284K (GAA⟶AAA)	*xdh* ←	selenium-dependent xanthine dehydrogenase
2,082,421														X														Δ999 bp		*[RS10080]–[RS10085]*	catechol 2,3-dioxygenase; multidrug ABC trans
2,114,057												X																C⟶T	G18S (GGT⟶AGT)	*RS10245* ←	GtrA family protein
2,123,718												X																C⟶T	R53C (CGC⟶TGC)	*RS10295* →	GntR family transcriptional regulator
2,181,891										X																		+A	coding (74/1269)	*RS10530* ←	exonuclease SbcCD subunit D
2,306,141																				X								C⟶T	intergenic (-14/+376)	*RS11200* ← / ← *RS11205*	MarR family regulator/YkuJ family protein
2,354,333							X																					4 bp⟶GAAA	intergenic (-96/+293)	*RS11435* ← / ← *tpx*	valine--tRNA ligase/thiol peroxidase
2,366,924																					X							T⟶A	intergenic (-60/+32)	*rbsK* ← / ← *RS11500*	ribokinase/substrate-binding protein
2,444,841														X														Δ1 bp	coding (269/1656)	*RS11840* →	peptide ABC transporter substrate-binding protein
2,572,276									X	X																		G⟶A	A464V (GCA⟶GTA)	*rny* ←	ribonuclease Y
2,627,715																								X				C⟶A	L1162F (TTG⟶TTT)	*rpoC* ←	RNA polymerase subunit beta prime
2,630,992												X		X														T⟶C	Y70C (TAT⟶TGT)	*rpoC* ←	RNA polymerase subunit beta prime
2,633,037															X													G⟶A	R649C (CGT⟶TGT)	*rpoB* ←	RNA polymerase subunit beta
2,633,525											X																	C⟶T	R486H (CGT⟶CAT)	*rpoB* ←	RNA polymerase subunit beta

FIG 1 Mutations in clones from experimental evolution. The clone cell shading indicates: pink, evolved at pH 4.8; violet, evolved at pH 7.0; blue, evolved at pH 9.0; cyan, biofilm evolution at pH 9.0. The mutation cell shading indicates: pink, *fusA* mutations; blue, mutations in *pstABC*, *pstB2*, and *pyrR*.

high proportion of nonsynonymous changes indicates the occurrence of adaptive selection (43). Another sign of adaptive selection is that two-thirds of the mutant genes are shared by at least two clones, despite the mutations being at different positions.

Acid-evolved *fusA* mutants are fusidate-sensitive at pH 7.0. In our acid-evolved clones, the gene that showed the most mutations encodes elongation factor G (*fusA*), which is an essential translation protein that is associated with virulence and biofilm formation (36, 44, 45). The ancestral strain OG1RF is resistant to fusidic acid and is associated with the *fusA* mutation C316A (2). We found an additional missense mutation in *fusA* in every acid-evolved clone as well as in four of our eight pH 7.0-evolved clones (Fig. 1). Six different missense mutations occurred in different strains. No *fusA* mutations were found in populations that evolved at high pH values. Two acid-evolved clones contained an additional mutation affecting a gene of unknown function, namely, RS05200, which encodes a helix-turn-helix protein. Another clone showed a missense mutation in *xdh* (xanthine dehydrogenase).

The mutant strains from the pH 4.8-evolved populations were tested for growth advantages during culture at low pH. (Fig. 2). At all three pH levels (pH 4.8, pH 7.0, pH 9.2), the growth curves for the mutants were indistinguishable from those of the ancestral strain. For all strains, the steepest rise for log-phase growth occurred at the optimal condition of pH 7.0 (panels B and E). Under the conditions tested, we saw no evidence of directional selection at low pH.

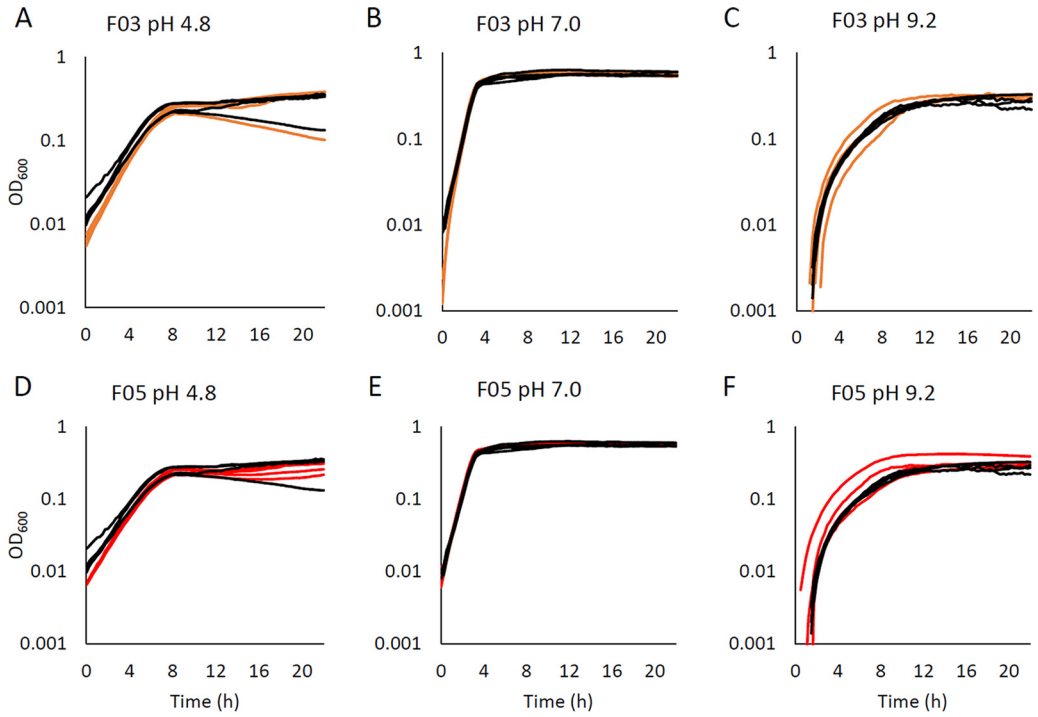

FIG 2 Acid-selected *fusA* mutants show no growth enhancement. *E. faecalis* clones were isolated after 500 generations of planktonic evolution (described under Materials and Methods) at pH 4.8. Each clone containing a single mutation in *fusA* was cultured for approximately 20 h at 37°C in BHI that was buffered at pH 4.8, at pH 7.0, or at pH 9.2. Then, 2 μL were inoculated into 200 μL at the same pH. Four representative curves are shown for each strain: F03 (*fusA*), orange lines (A–C); F05 (*fusA*), red lines (D–F); OG1RF (ancestor), black lines for all panels.

Since all our acid-evolved clones and four of the eight clones that were evolved at pH 7.0 showed an additional point mutation in *fusA*, we tested all of the clones for fusidate resistance, in comparison with the ancestor OG1RF (Fig. 3; Fig. S1). All clones containing a *fusA* mutation had lower fusidate resistance than did OG1RF. These included four clones in which the *fusA* mutation was the only change in the genome that was reported by the *breseq* pipeline (clones F03, F05, F06, and C01). In contrast, the clones lacking a *fusA* mutation (F08, F09, F10, C08) showed fusidate resistance that was indistinguishable from that of the ancestor. Each of the six different *fusA* mutations incurred a single amino-acid substitution at sites that were different from that of the OG1RF mutation (2). Thus, it appears that various kinds of changes in FusA structure can reverse the OG1RF resistance phenotype.

The evolved strains were also tested for changes in sensitivity to other antibiotics: rifampin, ampicillin, trimethoprim, erythromycin, gentamicin, norfloxacin, streptomycin, nalidixic acid, tetracycline, and chloramphenicol. None of these antibiotics revealed any difference in sensitivity between the evolved clones and the ancestral strain OG1RF.

Base-evolved populations had mutations in phosphate transport (*pst*) and metabolism (*pyr*). The base-evolved clones had the largest numbers of mutations, overall (Fig. 1). All but one of the eight strains from the pH 9.0 evolution showed a mutation in a gene involving phosphate metabolism: *pstB*, *pstB2* (both encoding a phosphate ATP-binding protein of an ABC transporter [46, 47]), and *pyrR* (encoding a bifunctional pyrimidine transcriptional regulator/uracil phosphoribosyltransferase [48–50]). A majority of these mutations were frameshift or nonsense codons that would knock out the gene. Each strain showed one mutation in one of these three genes. Several base-evolved clones had additional mutations. Four clones had deletions affecting *ccpA* (catabolite control protein A), and four clones had deletions in various subunits of *oppBCDF* (an oligopeptide ABC transporter). Two clones had missense mutations in an ArgR-family transporter, and another two clones had mutations in the septation protein FtsZ.

Several genes were mutated in populations that evolved at pH 7.0 and at pH 9.0. These included *opp1BCDR*, *ccpA*, *walK* (cell wall metabolism sensor histidine kinase), *rpoB*, and

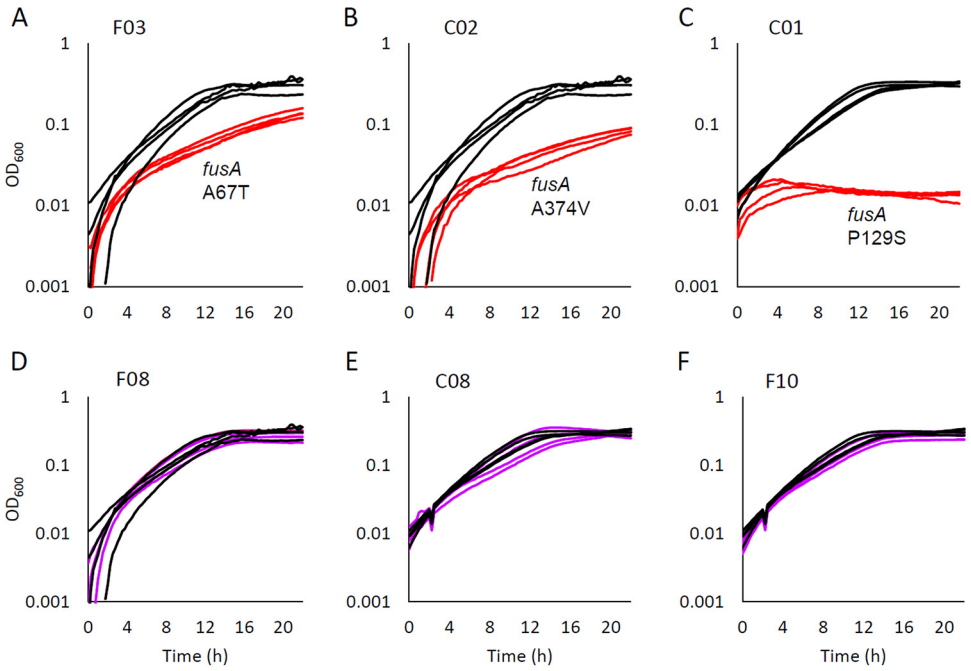

FIG 3 Evolved clones with *fusA* mutations lose resistance to fusidic acid. For each clone, eight replicate cultures were compared with replicates of the ancestor OG1RF. All were cultured with 400 μg/mL fusidic acid in BHI that was buffered at pH 7.0 at 37°C. (A–C) Clones evolved at pH 4.8 (red lines) show lower growth than does strain OG1RF (black lines). Endpoint growth was compared at 22 h by using two-tailed unpaired *t* tests ($P < 0.01$). (D–F) Clones evolved at pH 7.0 (purple lines) show growth rates that are indistinguishable from that of strain OG1RF (black lines).

rpoC (RNA polymerase subunits beta and beta prime). The only gene mutated solely in two pH 7.0-evolved clones was *rny* (RNase Y).

Biofilm evolution via bead transfer yields small-colony clones. The evolution experiment was modified to favor genetic variants that adhere to a bead forming a biofilm (31, 32). Cultures underwent four bead transfers over 6 days, generating approximately 25 to 50 doublings. The final populations were plated on BHI and inspected for variant phenotypes. No phenotypes were observed after evolution in acid (pH 4.8) or at pH 7.0, but the pH 9.0-evolved populations showed two colony-size morphs, one of which was small and one of which was large. Three small-colony clones that retained the phenotype upon reculturing were found: strains M02, M06, and M08 (Fig. 4). The relative sizes of their colonies, compared to those of the ancestor, OG1RF were approximately M02, 60%; M06, 30%; M08, 60%. The genomes of these clones were sequenced, and each revealed a single mutation (Fig. 1). The mutations affected the genes *pstB2* (M02), *pstC* (M06), and *pyrR* (M08).

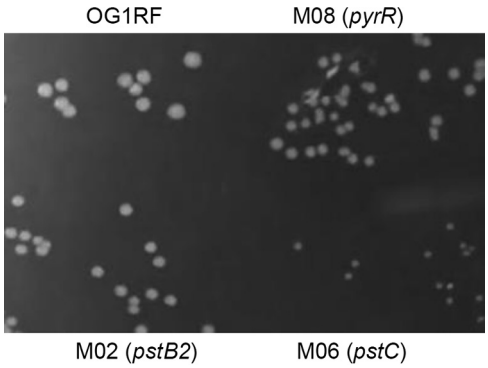

FIG 4 Small-colony phenotype of biofilm-evolved isolates. Each biofilm-evolved strain of *E. faecalis* OG1RF was streaked on BHI and cultured for approximately 20 h at 25°C and then for approximately 4 h at 37°C.

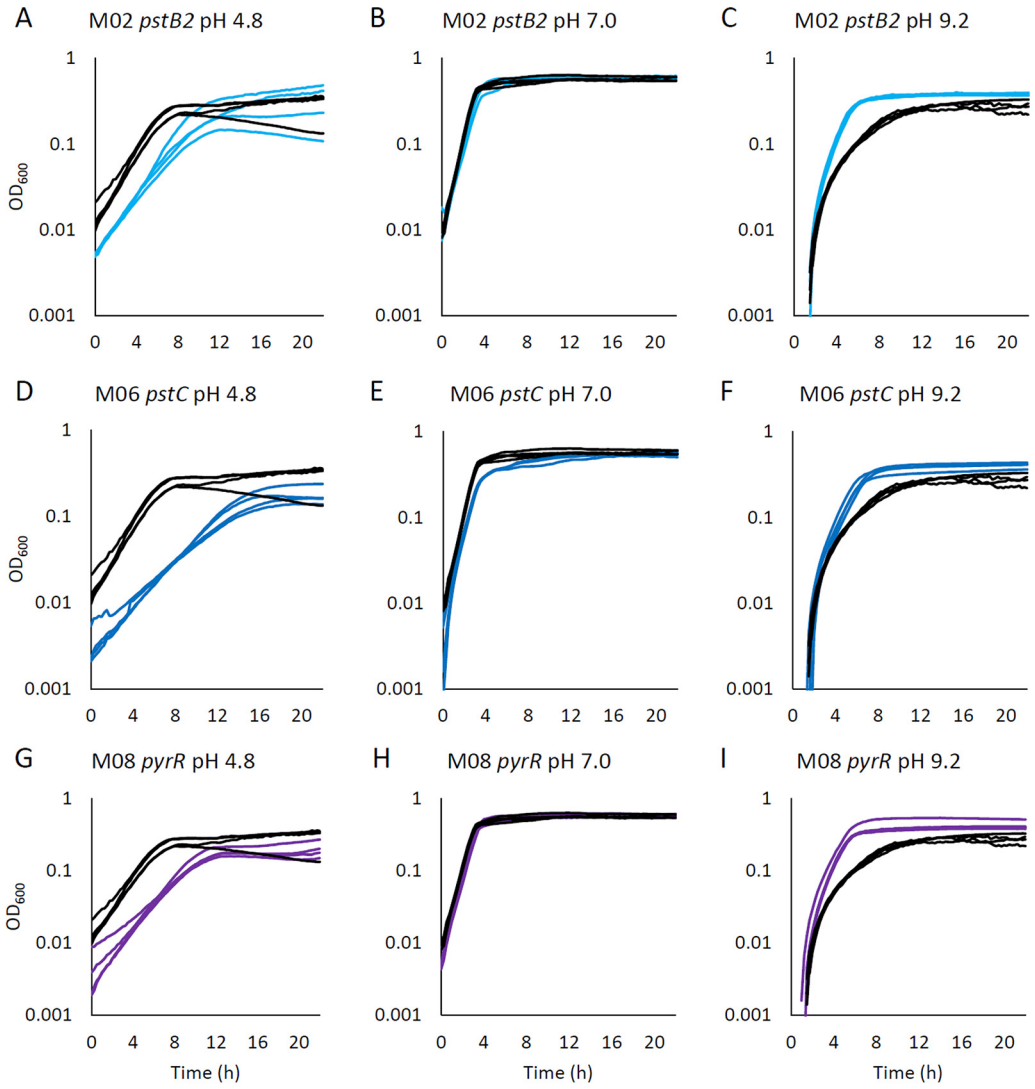

FIG 5 High pH-selected biofilm mutants show increased growth at high pH values and decreased growth at low pH values. The *E. faecalis* strains M02, M06, and M08 were isolated as small colonies from the bead-transfer biofilm evolution of *E. faecalis* OG1RF at pH 9.0 (described under Materials and Methods). Each clone was cultured for approximately 20 h at 37°C in BHI that was buffered at pH 4.8, at pH 7.0, or at pH 9.2. Then, 2 μL were inoculated into 200 μL of BHI that was buffered at the same pH. Four representative curves are shown for each strain: M02 (*pstB2*), cyan lines (A–C); M06 (*pstC*), blue lines (D–F); M08 (*pyrR*), violet lines (G–I); OG1RF (ancestor), black lines for all panels. Culture growth was compared at time 6 h by using two-tailed unpaired *t* tests ($P < 0.05$).

Base-evolved clones with *pst* and *pyr* mutations showed evidence of directional selection. We sought evidence for directional selection by observing the batch growth profiles for clones from populations that evolved at pH 4.8, pH 7.0, and pH 9.0. Each clone was cultured overnight in the three different pH-buffered media for physiological adaptation to each condition. The strongest evidence for directional selection was observed for the pH 9.0-evolved strains containing a mutation in one of the phosphate-related genes. Fig. 5 shows the growth curves for the biofilm pH 9.0-evolved strains that each contained one mutation that was detected by *breseq* in *pstB2* (M02), *pstC* (M06), and *pyrR* (M08). In each case, the log-phase growth (during approximately 0 to 7 h) was significantly lower at pH 4.8 for the mutant replicates than for the replicate curves of the ancestral strain OG1RF, and it was higher than that of the ancestor at pH 9.2 (significance was tested at 6 h, $P < 0.05$). No consistent selection effect was observed at pH 7.0. These observations are consistent with selection for a high pH-adaptive mutation following prolonged serial culture at a high pH value with a directional trade-off loss of growth rate at low pH values.

Similar evidence of base-adaptive selection was demonstrated for seven of the eight mutant clones that were obtained from high-pH planktonic evolution (Fig. S2). Only clone C10 showed a substantial decrease in growth. Of the eight base-evolved clones, all but clone C12 showed a mutation in *pst* or *pyrR* as well as mutations in other genes. All eight clones showed a small-colony phenotype on BHI media.

The mutations in phosphate transport that were favored at high pH may lead to a dependence on phosphate concentration. However, the amendment of the culture media with 10 mM or 50 mM phosphate did not significantly affect the growth curves of the evolved strains or of the ancestral strain, either at pH 4.8 or at pH 9.2.

DISCUSSION

The adaptability of *Enterococcus* bacteria to environmental stresses, such as acidic or basic conditions, is essential for the human microbiome as well as for soil and plant-associated communities (9, 17–22, 30, 51). However, few studies employ the approach of experimental evolution to examine stress factors under long-term adaptation. Most serial-culture studies of *Enterococcus* sp. focus on virulence or antibiotic resistance, rather than on environmental factors (34, 52).

We show that the experimental evolution of *E. faecalis* leads to distinct pH-dependent patterns of mutations (Fig. 1). In most cases, genes or operons with variants in multiple clones (which are the most likely to result from adaptation), are affected at only one end of the pH range; that is, under acidic or basic conditions, but not under both. This finding is important, as most studies of *Enterococcus* adaptation do not account for pH.

Each of the eight acid-adapted clones had one nonsynonymous codon replacement affecting elongation factor G. Five clones from different populations had alanine replaced by threonine, and the other clones had one of three different substitutions. Four of the eight populations evolving at pH 7.0 had a nonsynonymous substitution in *fusA*, but no *fusA* variants appeared at high pH. A possible explanation for this could be that a decrease in cell pH destabilizes the elongation factor G protein and that the mutations restore protein function. Although directional selection for acid adaptation was not shown under the conditions that were tested, the high frequency of *fusA* missense mutations argues for the occurrence of selection. Similarly, acid-dependent evolution in *E. coli* leads to mutations in amino-acid decarboxylases that are known to help pH regulation, although phenotypes have not been detected (25). The *E. faecalis* strain OG1RF is an important model organism for *Enterococcus* genetic analysis. Thus, our finding of the instability of the fusidate resistance phenotype should be noted.

The *fusA* mutations did show an important trade-off, namely, the loss of resistance to fusidic acid. This finding implies that *E. faecalis* growth at low pH, such as in dental biofilms and in the intestine (17, 51), could select against some forms of antibiotic resistance. Previously, acid (pH 5.5) increased the fusidate sensitivity of the clinical isolates of methicillin-resistant *Staphylococcus aureus* (53, 54). Fusidic acid resistance might incur a molecular trade-off with acid tolerance. For example, in *E. coli*, elongation factor G is stable between pH 7.5 and pH 9.0, but it is increasingly unstable at lower pH levels (55, 56). The low pH level may alter the protonation state of amino acid residues in the protein and thereby cause it to become unstable. The mutations we observe in the *fusA* gene could allow it to have a greater stability at lower pH levels, but at the expense of greater susceptibility to fusidic acid.

High pH effects on *Enterococcus* species are important for dental microbiomes because these bacteria can resist endodontic therapies involving the application of high-pH pastes, such as calcium hydroxide (20, 30). The basis of high-pH resistance is poorly understood, as several genes are upregulated at high pH values (21, 22). One of these genes, encoding the key septation protein FtsZ, had an amino-acid substitution in two of our high-pH clones (Fig. 1).

We show evidence for the directional selection of variants that knock out a component of the PstABC phosphate uptake system, which occurs in most cases via frame-shifting deletion or nonsense substitution (Fig. 1). Each *pst* mutation that we found

was associated with higher growth at high pH but lower growth at low pH (Fig. 5). The *pstC* mutant (strain M06) showed the smallest colonies (Fig. 4). This would make sense if *pstC* knocks out the entire phosphate uptake, whereas mutations in the *pstB* or *pstB2* redundant genes only partly cut phosphate uptake.

The growth rate change of *pst* and *pyrR* mutations led to visibly smaller colonies on BHI media. Although no change in antibiotic resistance was found under our conditions, in clinical studies, small-colony variants are associated with drug resistance and increased virulence (39, 40, 57). Mutations in *pst* genes are associated with clinical virulence (38) and altered antibiotic resistance (47). In soil and plant root communities, phosphate release is maximized at a pH below 7.0 (58, 59), and it has been proposed to contribute to bacterial pH regulation (60). In this model, phosphate release is inhibited at low pH and activated at high pH. Blocking phosphate uptake at high pH could enhance alkali-induced phosphate release.

The effect of *pyrR* loss and its relationship to phosphate is unclear. One possible connection to phosphate transport is the uracil phosphoribosyltransferase activity of this regulator (49). This enzyme reaction releases pyrophosphate and has a high optimum pH. Thus, it could be that the deletion of *pyrR* decreases phosphate release at high pH. In pathogenic staphylococci, *pyrR* is associated with biofilm formation and virulence (50, 61).

Additional mutated genes in the high-pH evolved population include two metabolic loci: the oligotransport operon *oppBCD* and the catabolite reculator *cppA*. Changes in these genes could enhance metabolism under the lowered energy condition of high pH, where the transmembrane pH difference is inverted and the proton potential consists solely of a charge difference (62). Overall, our study shows how *E. faecalis* exposure to an acid or a base can lead to evolutionary shifts with potential importance for host adaptation.

MATERIALS AND METHODS

Bacterial strains and culture media. All strains of *E. faecalis* are derivatives of the *E. faecalis* OG1RF (2) that was kindly provided by Barbara Murray. All evolving populations originated from the same overnight culture that was made from a single isolated colony. A portion of the original overnight culture was frozen for use as the ancestor in all future experiments.

For the evolution experiments, the strains were cultured in a pH-buffered brain heart infusion medium under BSL-2 conditions at 25°C. For growth curves, incubation was at 37°C. Buffers for experimental evolution included 100 mM homopiperazine-1,4-bis(2-ethanesulfonic acid) (HOMOPIPES, pK_a = 4.55) and 100 mM N-cyclohexyl-3-aminopropanesulfonic acid (CAPS, pK_a = 10.4). For some of the phenotype testing at pH 7.0, the buffer that was included in the growth medium was piperazine-N,N′-bis(2-ethanesulfonic acid) (PIPES, pKa = 6.8). The pH was adjusted by using KOH. The fusidic acid was from Millipore-Sigma. Some colony isolations were performed on tryptic soy agar (TSA). The bacterial cultures were regularly checked for contamination via microscopy.

Experimental evolution of planktonic cells. The serial culture was performed via dilution into deep well microplates daily or after two days (every sixth dilution). Eight serial cultures were maintained at each pH: pH 4.8, pH 7.0, and pH 9.0. For each dilution, 4 μL of the previous culture was transferred into 1,000 μL (1:250) of fresh medium. All media consisted of brain heart infusion media buffered with 0.1 M (each) CAPS HOMOPIPES that was adjusted with KOH to the appropriate pH. Two days of growth was assumed to yield approximately eight generations (doublings). All of the evolving populations were propagated to at least 500 generations. From every sixth dilution, 200 μL was combined with 100 μL of 50% glycerol and transferred to a deep well plate for storage at −80°C.

Once the evolved populations reached approximately 500 generations, each well was streaked on an individual plate of brain heart infusion agar (BHI) and cultured for 48 h. Two clones were chosen from each well population and were used to create individual overnight cultures in BCH. 2 μL of the first set of overnight solutions were used to inoculate 1 mL of fresh BCH overnight. A portion of each clone was converted to a freezer stock, and a portion was extracted for genomic DNA.

Experimental evolution of biofilms. Biofilm evolution was performed via serial bead transfer, based on the methods devised by Cooper and colleagues (31, 32). Four replicate populations of *E. faecalis* OG1RF were grown at 25°C in the presence of 7 mm white polystyrene beads that were suspended in 2 mL of BHI buffered with CAPS and HOMOPIPES, adjusted to the appropriate pH. The low-pH culture was performed at pH 4.8, the neutral pH culture was performed at 7.0, and the high-pH culture was performed at pH 9.0. Populations were selected for reversible surface attachment via the transfer of the white bead to a new test tube, where cells must adhere to a new black bead in order to persist. Each population with the beads was incubated for 48 h. This process was repeated by alternating the addition of white and black beads for a total of four serial dilutions. White and black beads were alternated to distinguish the previous biofilm from the newer colonized one.

At the end of the dilution series, each bead was placed in 1 mL BHI medium to wash off most of the planktonic cells and was then placed in 1 mL fresh BHI again and vortexed for 1 min. The vortexed

suspension was then plated on BHI agar plates and incubated for 48 h. The plates were then observed for novel colony morphologies.

Growth curves. From streaked TSA or BHI plates of approximately 500-generation evolution isolates, single colonies were picked for overnight culture in BCH buffered at the same pH as the subsequent microplate (pH 4.8, pH 7.0, or pH 9.2). 2 μL of an overnight culture of *E. faecalis* were transferred into sterile 96-well microplates with 200 μL (1:100) of BCH or other media with 100 mM HOMOPIPES and 100 mM CAPS, adjusted to the appropriate pH. The growth curves were performed on a SpectraMax microplate reader (Molecular Devices) at OD_{600}, with OD reads being taken every 15 min for 22 h. The comparison of batch growth was performed by using two-tailed unpaired *t* tests at standard intervals, postinoculation.

DNA sequence analysis. For the planktonic evolution cultures, DNA was extracted from one selected approximately 500-generation isolate of each well (24 isolates) as well as from the OG1RF(B) ancestral strain (2 isolates). The 24 sequenced clones were designated BF01-14 and C01-12. For the biofilm evolution at pH 9.0, the final biofilm bead suspensions were streaked on BHI agar. After 48 h, one large colony and one small colony variant (SCV) were isolated from each plate and were separately streaked on new BHI plates. The isolates were plated on BHI two more times to ensure the persistence of the growth phenotype. Three large-colony isolates (M1, M5, M7) and three small-colony isolates (M2, M6, M8) were selected for DNA preparation and sequencing.

Genomic DNA was extracted using a MasterPure Gram Positive DNA Purification Kit. The purity and the concentrations of DNA were determined using a NanoDrop 2000 spectrophotometer (Thermo Fisher Scientific). DNA was sequenced by Admera Health (South Plainfield, NJ). Library preparation was performed using a NexteraXT Library Kit (Illumina, CA, USA). Sequencing was performed using an Illumina NovaSeq (Illumina, CA, USA) with a read length of 150 bp for 40 million paired-end reads.

Mutations were called from the DNA sequences by alignment to the *E. faecalis* OG1RF reference sequence with the NCBI accession number NC_017316.1, using the *breseq* version 0.36.1 resequencing pipeline (41, 42). The resulting genomic data had approximately 300-fold coverage. Our lab stock of OG1RF, which was the ancestor for all of the evolution experiments, showed two differences from the reference that appeared in all of our evolved clones: the insertion of A at genome position 260,670, which caused a frameshift in gene RS01405 (acyl-ACP thioesterase) and a T deletion at position 2,108,103 within an intergenic region.

Data availability. All of the sequence data are deposited at NCBI, SRA PRJNA933188.

SUPPLEMENTAL MATERIAL

Supplemental material is available online only.

SUPPLEMENTAL FILE 1, PDF file, 0.4 MB.

ACKNOWLEDGMENTS

This work was supported by the National Science Foundation award MCB-1923077. We thank Daniel Barich for the assistance with the computing and the statistics. We are grateful to Kelli Palmer for helpful advice on *E. faecalis*.

B.A.F. performed the planktonic evolution, and A.W. performed the biofilm evolution. B.A.F. and A.W. both drafted the manuscript. B.A.F., A.W., and Z.S. conducted the growth curves. J.L.S. conceived the study, mentored the students, and completed the manuscript.

REFERENCES

1. Arias CA, Murray BE. 2012. The rise of the Enterococcus: beyond vancomycin resistance. Nat Rev Microbiol 10:266–278. https://doi.org/10.1038/nrmicro2761.
2. Bourgogne A, Garsin DA, Qin X, Singh KV, Sillanpaa J, Yerrapragada S, Ding Y, Dugan-Rocha S, Buhay C, Shen H, Chen G, Williams G, Muzny D, Maadani A, Fox KA, Gioia J, Chen L, Shang Y, Arias CA, Nallapareddy SR, Zhao M, Prakash VP, Chowdhury S, Jiang H, Gibbs RA, Murray BE, Highlander SK, Weinstock GM. 2008. Large scale variation in Enterococcus faecalis illustrated by the genome analysis of strain OG1RF. Genome Biol 9:R110. https://doi.org/10.1186/gb-2008-9-7-r110.
3. Lebreton F, Willems RJL, Gilmore MS. 2014. Enterococcus diversity, origins in nature, and gut colonization. Enterococci: from commensals to leading causes of drug resistant infection. http://www.ncbi.nlm.nih.gov/pubmed/24649513.
4. Dubin K, Pamer EG. 2017. Enterococci and their interactions with the intestinal microbiome. Microbiol Spectr 5:5–6. https://doi.org/10.1128/microbiolspec.BAD-0014-2016.
5. Švec P, Vandamme P, Bryndová H, Holochová P, Kosina M, Mašlaňová I, Sedláček I. 2012. Enterococcus plantarum sp. nov., isolated from plants. Int J Syst Evol Microbiol 62:1499–1505. https://doi.org/10.1099/ijs.0.033357-0.
6. García-Solache M, Rice LB. 2019. The enterococcus: a model of adaptability to its environment. Clin Microbiol Rev 32. https://doi.org/10.1128/CMR.00058-18.
7. Gardini F, Martuscelli M, Caruso MC, Galgano F, Crudele MA, Favati F, Guerzoni ME, Suzzi G. 2001. Effects of pH, temperature and NaCl concentration on the growth kinetics, proteolytic activity and biogenic amine production of Enterococcus faecalis. Int J Food Microbiol 64:105–117. https://doi.org/10.1016/S0168-1605(00)00445-1.
8. Morandi S, Brasca M, Alfieri P, Lodi R, Tamburini A. 2005. Influence of pH and temperature on the growth of Enterococcus faecium and Enterococcus faecalis. Lait 85:181–192. https://doi.org/10.1051/lait:2005006.
9. Gaca AO, Lemos JA. 2019. Adaptation to adversity: the intermingling of stress tolerance and pathogenesis in Enterococci. Microbiol Mol Biol Rev 83. https://doi.org/10.1128/MMBR.00008-19.
10. Mchugh CP, Zhang P, Michalek S, Eleazer PD. 2004. pH required to kill Enterococcus faecalis in vitro.
11. Weckwerth PH, Zapata RO, Vivan RR, Tanomaru-Filho M, Maliza AGA, Duarte MAH. 2013. In vitro alkaline pH resistance of Enterococcus faecalis. Braz Dent J 24:474–476. https://doi.org/10.1590/0103-6440201301731.
12. dos Santos LDR, Furlan JPR, Gallo IFL, Ramos MS, Savazzi EA, Stehling EG. 2021. Occurrence of multidrug-resistant Enterococcus faecium isolated from environmental samples. Lett Appl Microbiol 73:237–246. https://doi.org/10.1111/lam.13508.
13. Ramos S, Silva V, Dapkevicius M, Igrejas G, Poeta P. 2020. Enterococci, from harmless bacteria to a pathogen. Microorganisms 8:1118. MDPI AG. https://doi.org/10.3390/microorganisms8081118.

14. Sen S, Saha T, Bhattacharya S, Mondal N, Ghosh W, Chakraborty R. 2020. Draft genome sequences of two boron-tolerant, arsenic-resistant, Gram-positive bacterial strains, Lysinibacillus sp. OL1 and Enterococcus sp. OL5, isolated from boron-fortified cauliflower-growing field soils of northern West Bengal, India. https://doi.org/10.1128/MRA.
15. Singhal N, Maurya AK, Mohanty S, Kumar M, Virdi JS. 2019. Evaluation of bile salt hydrolases, cholesterol-lowering capabilities, and probiotic potential of Enterococcus faecium isolated from rhizosphere. Front Microbiol 10. https://doi.org/10.3389/fmicb.2019.01567.
16. Yu Z, Shi D, Liu W, Meng Y, Meng F. 2020. Metabolome responses of Enterococcus faecium to acid shock and nitrite stress. Biotechnol Bioeng 117:3559–3571. https://doi.org/10.1002/bit.27497.
17. Flahaut S, Hartke A, Giard J, Benachour A, Boutibonnes P, Auffray Y. 1996. Relationship between stress response towards bile salts, acid and heat treatment in Enterococcus faecalis. FEMS Microbiol Lett 138:49–54. https://doi.org/10.1111/j.1574-6968.1996.tb08133.x.
18. Benachour A, Muller C, Dabrowski-Coton M, Le Breton Y, Giard JC, Rincé A, Auffray Y, Hartke A. 2005. The Enterococcus faecalis SigV protein is an extracytoplasmic function sigma factor contributing to survival following heat, acid, and ethanol treatments. J Bacteriol 187:1022–1035. https://doi.org/10.1128/JB.187.3.1022-1035.2005.
19. Salze M, Giard JC, Riboulet-Bisson E, Hain T, Rincé A, Muller C. 2020. Identification of the general stress stimulon related to colonization in Enterococcus faecalis. Arch Microbiol 202:233–246. https://doi.org/10.1007/s00203-019-01735-8.
20. Evans M, Davies JK, Sundqvist G, Figdor D. 2002. Mechanisms involved in the resistance of Enterococcus faecalis to calcium hydroxide. Int Endod J 35:221–228. https://doi.org/10.1046/j.1365-2591.2002.00504.x.
21. Ran S, He Z, Liang J. 2013. Survival of Enterococcus faecalis during alkaline stress: changes in morphology, ultrastructure, physiochemical properties of the cell wall and specific gene transcripts. Arch Oral Biol 58:1667–1676. https://doi.org/10.1016/j.archoralbio.2013.08.013.
22. Ran S, Liu B, Jiang W, Sun Z, Liang J. 2015. Transcriptome analysis of Enterococcus faecalis in response to alkaline stress. Front Microbiol 6. https://doi.org/10.3389/fmicb.2015.00795.
23. Flahaut S, Hartke A, Giard J-C, Auffray Y. 1997. Alkaline stress response in Enterococcus faecalis: adaptation, cross-protection, and changes in protein synthesis. Appl Environ Microbiol 63:812–814. https://doi.org/10.1128/aem.63.2.812-814.1997.
24. Harden MM, He A, Creamer K, Clark MW, Hamdallah I, Martinez KA, Kresslein RL, Bush SP, Slonczewski JL. 2015. Acid-adapted strains of Escherichia coli K-12 obtained by experimental evolution. Appl Environ Microbiol 81:1932–1941. https://doi.org/10.1128/AEM.03494-14.
25. He A, Penix SR, Basting PJ, Griffith JM, Creamer KE, Camperchioli D, Clark MW, Gonzales AS, Erazo JSC, George NS, Bhagwat AA, Slonczewski JL. 2017. Acid evolution of Escherichia coli K-12 eliminates amino acid decarboxylases and reregulates catabolism. Appl Environ Microbiol 83:e00442-17. https://doi.org/10.1128/AEM.00442-17.
26. Creamer KE, Ditmars FS, Basting PJ, Kunka KS, Hamdallah IN, Bush SP, Scott Z, He A, Penix SR, Gonzales AS, Eder EK, Camperchioli DW, Berndt A, Clark MW, Rouhier KA, Slonczewski JL. 2017. Benzoate- and salicylate-tolerant strains of Escherichia coli K-12 lose antibiotic resistance during laboratory evolution. Appl Environ Microbiol 83:e02736. https://doi.org/10.1128/AEM.02736-16.
27. Moore JP, Li H, Engmann ML, Bischof KM, Kunka KS, Harris ME, Tancredi AC, Ditmars FS, Basting PJ, George NS, Bhagwat AA, Slonczewski L. 2019. Inverted regulation of multidrug efflux pumps, acid resistance, and porins in benzoate-evolved Escherichia coli K-12. Appl Environ Microbiol 85:e00966-19. https://doi.org/10.1128/AEM.00966-19.
28. Hamdallah I, Torok N, Bischof KM, Majdalani N, Chadalavada S, Mdluli N, Creamer KE, Clark M, Holdener C, Basting PJ, Gottesman S, Slonczewski JL. 2018. Experimental evolution of Escherichia coli K-12 at high pH and RpoS induction. Appl Environ Microbiol 84:e00520. https://doi.org/10.1128/AEM.00520-18.
29. Johnson MD, Bell J, Clarke K, Chandler R, Pathak P, Xia Y, Marshall RL, Weinstock GM, Loman NJ, Winn PJ, Lund PA. 2014. Characterization of mutations in the PAS domain of the EvgS sensor kinase selected by laboratory evolution for acid resistance in Escherichia coli. Mol Microbiol 93:911–927. https://doi.org/10.1111/mmi.12704.
30. Nakajo K, Komori R, Ishikawa S, Ueno T, Suzuki Y, Iwami Y, Takahashi N. 2006. Resistance to acidic and alkaline environments in the endodontic pathogen Enterococcus faecalis. Oral Microbiol Immunol 21:283–288. https://doi.org/10.1111/j.1399-302X.2006.00289.x.
31. Martin M, Hölscher T, Dragoš A, Cooper VS, Kovács ÁT. 2016. Laboratory evolution of microbial interactions in bacterial biofilms. J Bacteriol 198:2564–2571. https://doi.org/10.1128/JB.01018-15.
32. Poltak SR, Cooper VS. 2011. Ecological succession in long-term experimentally evolved biofilms produces synergistic communities. ISME J 5:369–378. https://doi.org/10.1038/ismej.2010.136.
33. Khan A, Davlieva M, Panesso D, Rincon S, Miller WR, Diaz L, Reyes J, Cruz MR, Pemberton O, Nguyen AH, Siegel SD, Planet PJ, Narechania A, Latorre M, Rios R, Singh K, Ton-That H, Garsin DA, Tran TT, Shamoo Y, Arias CA. 2019. Antimicrobial sensing coupled with cell membrane remodeling mediates antibiotic resistance and virulence in Enterococcus faecalis. Proc Natl Acad Sci U S A 116:26925–26932. https://doi.org/10.1073/pnas.1916037116.
34. Sun Y, Lu H, Zhang X, Wu Q, Bi W, Liu H, Cao J, Zhou T. 2018. Phenotype and genotype alteration during adaptive evolution of Enterococcus faecalis to antimicrobials. Infect Genet Evol 62:80–85. https://doi.org/10.1016/j.meegid.2018.03.029.
35. Guo X, Peisker K, Bäckbro K, Chen Y, Koripella RK, Mandava CS, Sanyal S, Selmer M. 2012. Structure and function of FusB: an elongation factor G-binding fusidic acid resistance protein active in ribosomal translocation and recycling. Open Biol 2:120016. https://doi.org/10.1098/rsob.120016.
36. Gupta SK, Pfeltz RF, Wilkinson BJ, Gustafson JE. 2022. Transcriptomic and metabolomic analysis of a fusidic acid-selected fusA mutant of Staphylococcus aureus. Antibiotics 11:1051. https://doi.org/10.3390/antibiotics11081051.
37. Durango H, Morales H, Murillo E. 2021. Evaluation of the virulence factor prole of avian pathogenic Escherichia coli in clinical isolates of avian samples in Caloto, Cauca, Colombia. https://doi.org/10.21203/rs.3.rs-1184472/v1.
38. Lieberman MT, Van Tyne D, Dzink-Fox JA, Ma EJ, Gilmore MS, Fox JG. 2018. Long-term colonization dynamics of Enterococcus faecalis in implanted devices in research macaques. Appl Environ Microbiol 84. https://doi.org/10.1128/AEM.01336-18.
39. Höring S, Sobotta K, Schneider S, Löffler B, Rödel J. 2019. Dwarfs in disguise: multiple spinal abscesses and spondylodiscitis caused by an Enterococcus faecium small-colony variant. Access Microbiol 1. https://doi.org/10.1099/acmi.0.000012.
40. Proctor RA, von Eiff C, Kahl BC, Becker K, McNamara P, Herrmann M, Peters G. 2006. Small colony variants: a pathogenic form of bacteria that facilitates persistent and recurrent infections. Nat Rev Microbiol 4:295–305. https://doi.org/10.1038/nrmicro1384.
41. Deatherage DE, Barrick JE. 2014. Identification of mutations in laboratory-evolved microbes from next-generation sequencing data using breseq. Methods Mol Biol 1151:165–188. https://doi.org/10.1007/978-1-4939-0554-6_12.
42. Barrick JE, Colburn G, Deatherage DE, Traverse CC, Strand MD, Borges JJ, Knoester DB, Reba A, Meyer AG. 2014. Identifying structural variation in haploid microbial genomes from short-read resequencing data using breseq. BMC Genomics 15:1039. https://doi.org/10.1186/1471-2164-15-1039.
43. Yang Z, Bielawski JP. 2000. Statistical methods for detecting molecular adaptation. Trends Ecol Evol 15:496–503. https://doi.org/10.1016/s0169-5347(00)01994-7.
44. Tokmakova IP, Ryabchenko LE, Gerasimova TV, Kameneva SV, Yanenko AS. 2017. Mutations in the fusA gene encoding elongation factor G in the Coryneform bacterium lead to increased lysine production. Appl Biochem Microbiol 53:781–785. https://doi.org/10.1134/S0003683817080075.
45. Qayyum S, Sharma D, Bisht D, Khan AU. 2019. Identification of factors involved in Enterococcus faecalis biofilm under quercetin stress. Microb Pathog 126:205–211. https://doi.org/10.1016/j.micpath.2018.11.013.
46. Maddalo G, Chovanec P, Stenberg-Bruzell F, Nielsen HV, Jensen-Seaman MI, Ilag LL, Kline KA, Daley DO. 2011. A reference map of the membrane proteome of Enterococcus faecalis. Proteomics 11:3935–3941. https://doi.org/10.1002/pmic.201100103.
47. Bhardwaj P, Islam MZ, Kim C, Nguyen UT, Palmer KL. 2021. ddcP, pstB, and excess D-lactate impact synergism between vancomycin and chlorhexidine against Enterococcus faecium 1,231,410. PLoS One 16:e0249631. https://doi.org/10.1371/journal.pone.0249631.
48. Copin R, Sause WE, Fulmer Y, Balasubramanian D, Dyzenhaus S, Ahmed JM, Kumar K, Lees J, Stachel A, Fisher JC, Drlica K, Phillips M, Weiser JN, Planet PJ, Uhlemann AC, Altman DR, Sebra R, van Bakel H, Lighter J, Torres VJ, Shopsin B. 2019. Sequential evolution of virulence and resistance during clonal spread of community-acquired methicillin-resistant Staphylococcus aureus. Proc Natl Acad Sci U S A 116:1745–1754. https://doi.org/10.1073/pnas.1814265116.
49. Ghim S-Y, Kim CC, Bonner ER, D'elia JN, Grabner GK, Switzer RL. 1999. The Enterococcus faecalis pyr operon is regulated by autogenous transcriptional

attenuation at a single site in the 5′ leader. J Bacteriol 181:1324–1329. https://doi.org/10.1128/JB.181.4.1324-1329.1999.
50. Wang Q, Sun FJ, Liu Y, Xiong LR, Xie LL, Xia PY. 2010. Enhancement of biofilm formation by subinhibitory concentrations of macrolides in icaADBC-positive and -negative clinical isolates of Staphylococcus epidermidis. Antimicrob Agents Chemother 54:2707–2711. https://doi.org/10.1128/AAC.01565-09.
51. Belli WA, Marquis RE. 1991. Adaptation of Streptococcus mutans and Enterococcus hirae to acid stress in continuous culture. Appl Environ Microbiol 57:1134–1138. https://doi.org/10.1128/aem.57.4.1134-1138.1991.
52. Miller C, Kong J, Tran TT, Arias CA, Saxer G, Shamoo Y. 2013. Adaptation of Enterococcus faecalis to daptomycin reveals an ordered progression to resistance. Antimicrob Agents Chemother 57:5373–5383. https://doi.org/10.1128/AAC.01473-13.
53. Biedenbach DJ, Rhomberg PR, Mendes RE, Jones RN. 2010. Spectrum of activity, mutation rates, synergistic interactions, and the effects of pH and serum proteins for fusidic acid (CEM-102). Diagn Microbiol Infect Dis 66:301–307. https://doi.org/10.1016/j.diagmicrobio.2009.10.014.
54. Lemaire S, Van Bambeke F, Pierard D, Appelbaum PC, Tulkens PM. 2011. Activity of fusidic acid against extracellular and intracellular Staphylococcus aureus: influence of pH and comparison with linezolid and clindamycin. Clinical Infectious Diseases 52:S493–S503. https://doi.org/10.1093/cid/cir165.
55. Sander G, Parlato G, Crechet J-, Nagel K, Parmeggiani A. 1978. Regulation of turnover GTPase activity of elongation factor G: the 30-S-coupled and 30-S-uncoupled reactions: coordinated effects of cations, pH and polyamines. Eur J Biochem 86:555–563. https://doi.org/10.1111/j.1432-1033.1978.tb12339.x.
56. Kaziro Y, Inoue-Yokosawa N, Kawakita M. 1972. Studies on polypeptide elongation factor from E. coli I. Crystalline factor G. J Biochem.
57. Thieme L, Klinger-Strobel M, Hartung A, Stein C, Makarewicz O, Pletz MW. 2018. In vitro synergism and anti-biofilm activity of ampicillin, gentamicin, ceftaroline and ceftriaxone against Enterococcus faecalis. J Antimicrob Chemother 73:1553–1561. https://doi.org/10.1093/jac/dky051.
58. Penn CJ, Camberato JJ. 2019. A critical review on soil chemical processes that control how soil pH affects phosphorus availability to plants. Agriculture (Switzerland) 9:120. https://doi.org/10.3390/agriculture9060120.
59. Arai Y, Sparks D. 2007. Phosphate reaction dynamics in soils and soil components: a multiscale approach. Advances in Agronomy 94:135–179. https://doi.org/10.1016/S0065-2113(06)94003-6.
60. Bond PL, Keller J, Blackall LL. 1999. Anaerobic phosphate release from activated sludge with enhanced biological phosphorus removal. A possible mechanism of intracellular pH control. Biotechnol Bioeng 63:507–515. https://doi.org/10.1002/(SICI)1097-0290(19990605)63:5%3C507::AID-BIT1%3E3.0.CO;2-A.
61. Beenken KE, Dunman PM, McAleese F, Macapagal D, Murphy E, Projan SJ, Blevins JS, Smeltzer MS. 2004. Global gene expression in Staphylococcus aureus biofilms. J Bacteriol 186:4665–4684. https://doi.org/10.1128/JB.186.14.4665-4684.2004.
62. Kakinuma Y. 1998. Inorganic cation transport and energy transduction in Enterococcus hirae and other Streptococci. Microbiol Mol Biol Rev 62:1021–1045. https://doi.org/10.1128/MMBR.62.4.1021-1045.1998.